

Single-Shot Partial-Fourier Spiral Imaging

B. J. Wilm¹, C. Barmet¹, M. Guerquin-Kern^{1,2}, M. Haerberlin³, and K. P. Pruessmann¹

¹Institute for Biomedical Engineering, University and ETH Zurich, Zurich, Zurich, Switzerland, ²Biomedical Imaging Group, EPFL Lausanne, Lausanne, Vaude, Switzerland, ³Institute for Biomedical Engineering, University and ETH Zurich, Zurich, Switzerland

Introduction: Compared to other k-space sampling strategies, spiral trajectories stand out in many respects. They allow for the shortest echo times, provide the highest SNR efficiency, achieve a uniform point-spread function and pose a well-conditioned reconstruction problem for parallel imaging when using circular coil-arrays such as typically applied for MRI of the brain. Single-shot spiral imaging is arguably the most efficient way to cover k-space, and could increase the achievable temporal resolution in dynamic MRI series and robustness against motion.

Despite these advantages, spiral k-space trajectories are rarely used in clinics. The main reasons are its vulnerability to gradient timing imperfections and static B₀ off-resonance. The latter effect scales with the acquisition duration and can therefore be addressed with parallel imaging as well as Partial Fourier imaging. Partial Fourier imaging exploits the fact that for a purely real magnetization in the object its k-space representation is complex-symmetric, meaning that $\sigma(\mathbf{k}) = \sigma(-\mathbf{k})^*$, where $\sigma(\mathbf{k})$ depicts the signal acquired at the k-space position \mathbf{k} , and * denotes complex conjugation. Therefore in theory the k-space can be asymmetrically undersampled by a factor of two without loss of information, if the object phase is known. However, even for short interleaved spiral acquisitions the use of Partial Fourier imaging has not been shown so far.

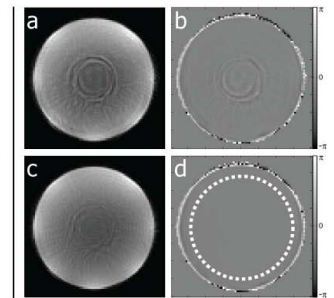
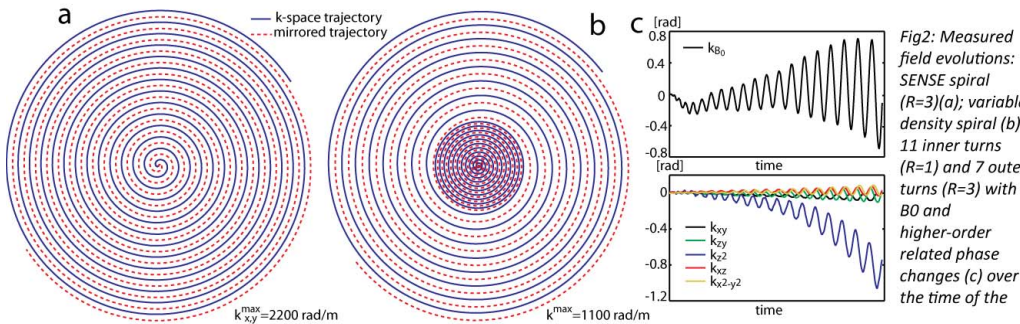


Fig3: Magnitude (a,c) and phase images (b,d) with (c,d) and without PF.

Since the recent invent of magnetic field monitoring [1,2],

precise knowledge of the actual encoding fields can be acquired simultaneously with the imaging data. The encoding fields include B₀ drifts, k-space trajectory as well as dynamic higher-order field information. In this work the provided information serves as the basis to higher-order image reconstruction [3]. In this work, Partial Fourier imaging is extended to higher-order fields and tested in-vitro and in-vivo.

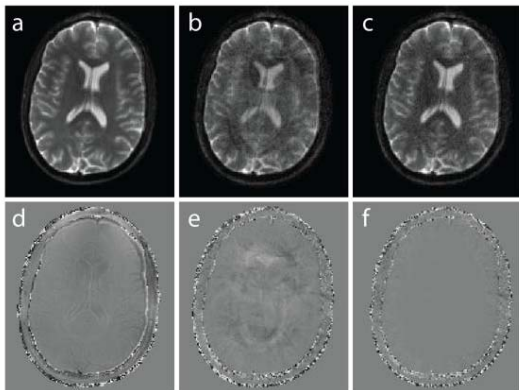


Fig4 Magnitude (a) and phase (b) images of an interleaved spiral R=1. Single-shot (R=6) spiral magnitude (b,d) and phase (e,f) images with (c,f) and without (b,e) PF.

Theory: An SNR optimal MR image reconstruction can be performed by solving the forward equation

$$\rho = (E^H \Psi^{-1} E)^{-1} E^H \Psi^{-1} \sigma \quad (1)$$

where ρ is the unknown vector of object pixels, σ is the acquired signal (possibly containing data from several coils) and Ψ is the noise covariance matrix [4]. The encoding matrix E can be written as

$$E_{(\nu,\kappa),\lambda} = s_\nu(\mathbf{r}_\lambda) e^{i\phi(\mathbf{r}_\lambda, t_\kappa)}$$

with ν, λ, κ counting the coil sensitivities s , grid points \mathbf{r} and time points t respectively. For computational efficiency Eq. 1 is solved iteratively by the conjugate gradient (CG) method. To incorporate partial Fourier encoding, the algorithm is adjusted (Fig 1) to penalize non-zero phase after demodulation with a phase estimate φ by multiplication with \mathbf{p}^* , where $\mathbf{p} = e^{i\varphi}$ [5]. The degree of penalization can be adjusted by the scalar α . Alternatively we propose to choose α as a mask which enables to exclude penalization of pixels where the phase is unreliably defined such as at the image borders.

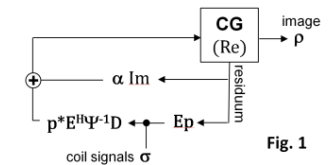


Fig. 1

Methods: Image data of a spherical phantom and in-vivo brain was acquired on a 3T Achieva system (Philips Healthcare, The Netherlands) using a 4-element head coil array. In scans the

field information (Fig. 1) was simultaneously acquired using a 3rd order concurrent monitoring setup [2] based on ¹⁹F-NMR probes. In the phantom a single-shot variable density spiral (Fig 1b) gradient echo sequence (TE=3 ms, readout dur.=25 ms, k_{max}=1100 rad/m, FOV=23cm, R=3) was acquired. In-vivo two spiral spin-echo EPI scans were acquired (Fig. 1a) (TE=50ms, readout dur. =18.5ms, k_{max}=1050rad/m, FOV=23cm) SENSE reduction factor of R≈1 and R=6 (single-shot). For both, the in-vivo and the phantom experiments the same slice was additionally acquired with two Cartesian gradient echo scans (TE=3.0 ms/3.6 ms, FOV=230, matrix=1.8 mm²).

In a first step the Cartesian gradient echo images were reconstructed without Partial Fourier. From these data the B₁-coil-sensitivity maps as well as a B₀-map were calculated. For the phantom scan a low-resolution phase map was extracted from the densely sampled k-space. The in-vivo phase map was obtained from the fully sampled spin-echo scan. Finally the B₀, B₁ and phase maps served as an input for the PF reconstruction. The amount of penalization α was heuristically set to 0.6 in the central part of the object, and 0 outside. For comparison the objects were also reconstructed with SENSE, but without Partial Fourier encoding.

Results: For the non-PF reconstructed images (Figs.3a,4b) residual fold-over artifacts are visible along with disturbance in the corresponding phase images (Figs. 3b,4e), while phantom (Fig 3) and in-vivo (Fig 4) geometry is reflected faithfully when incorporating Partial Fourier encoding (Fig 3c, 4c).

Discussion and Conclusion: The first application of partial Fourier encoding to spiral imaging was shown. Using only 4 receive channels a 6-fold undersampled single-shot in-vivo images without aliasing artifacts was reconstructed. Auto-calibrated PF was demonstrated with single-shot variable density spirals. The high image quality and resolution is attributed to the shortened readout duration and the accurate description of the encoding process which was incorporated into the higher-order image reconstruction.

References: [1] Barmet, MRM 60:187–197. [2] Barmet et al. ISMRM2010,216. [3] Wilm et al., MRM (in press).

[4] Pruessmann et al., MRM46:638. [5] Bydder et al. MRM 53:1393.